Experimental comparison of constitutive models for magnetorheological fluids under different conditions

Haopeng Li[1,2] **Ilari Jönkkäri**[2] **Essi Sarlin**[2] **Fei Chen**[1*]

[1] School of Mechatronic Engineering, China University of Mining and Technology, No.1, Daxue Road, Tongshan Zone, Xuzhou, Jiangsu Province 221116, P.R.China

[2] Faculty of Engineering and Natural Sciences, Tampere University, Korkeakoulunkatu 6, 33720 Tampere, Finland

*Corresponding author: Fei Chen (cfcumtxz@126.com)

Braz J Phys (2021). https://doi.org/10.1007/s13538-021-00989-2

Abstract: The accurate prediction of the viscosity and shear stress for magnetorheological (MR) fluids provides the basis for the preparation of MR fluids and the design of MR devices, where a proper model is a key. How to quickly choose an appropriate model to describe its rheological properties is important for the application of MR fluids. In this work, MR fluids with different mass fractions are prepared and their apparent viscosities and shear stresses are measured under different magnetic fields and shear rates. The obtained rheological parameters are fitted by the Bingham model, the Herschel-Bulkley model and the Casson model to evaluate their fitting effects. It is found that the MR fluid can be regarded as a Newtonian fluid only if its mass fraction is less than 30 wt% and there is no magnetic field. The shear thinning effect is the main cause of the constitutive model errors and it is more likely to occur for the MR fluids with higher mass fractions but increasing magnetic field strength will inhibit it. However, the shear thinning effect caused by the high-rate shear is even stronger than the inhibition through increasing magnetic field strength. The highest shear yield stress is obtained with the Bingham model, followed by the Carson model and finally the Herschel-Bulkley model. This work provides a guidance to accurately predict the shear stress of MR fluids through a suitable constitutive model.

Keywords: magnetorheological fluids, constitutive model, particle concentration, magnetic field strength, shear rate

1. Introduction

Magnetorheological (MR) fluid is a smart material that has been widely applied to vibration isolation[1], power transmission[2], polishing[3] and other applications [4, 5]. It can change from a fluid to a semi-solid under an applied magnetic field, which is called the MR effect. Shear stress is the most important mechanical parameter for MR fluids, which indicates how much force MR fluids can transfer. The shear stress is closely related to the factors such as particle material[6], particle concentration[7] and magnetic field strength[8], among others. A model that can describe the shear stress of MR fluids accurately is important for the preparation of MR fluids, as well as the selection of MR devices. In this regard, scholars are committed to finding a suitable model to describe the properties of MR fluids. Several models, such as the Biviscous model[9], the Eyring model[10], the Papanastasiou model[11], the Mizrahi–Berk model[12, 13], the Robertson-Stiff model[14] and the Rosensweig model[15], have been proposed, but the Bingham model[16], the Herschel-Bulkley model[17] and the Casson model[18] are the most

commonly used, which is originally employed to describe the properties of non-Newtonian fluids. The Bingham model evolves from the Newtonian fluid model and its constitutive equation is

$$\tau = \tau_0 + \eta_0 \dot{\gamma} \quad (\tau \geq \tau_0) \quad (1)$$

where τ_0 is the shear yield stress of the MR fluid under the applied magnetic field, η_0 is the dynamic viscosity, and $\dot{\gamma}$ is the shear rate. The Bingham model assumes that the shear stress of MR fluids increases linearly with the shear rate after yielding, where the viscosity remains constant like Newtonian fluids. Different from the Bingham model, the Herschel-Bulkley model is derived from the power-law fluid model [19]. Its constitutive equation is

$$\tau = \tau_0 + k\dot{\gamma}^n \quad (\tau \geq \tau_0) \quad (2)$$

where k is the flow consistency coefficient and n is the flow behavior index. The fluid is Newtonian if n=1, shear thinning if n<1 and shear thickening if n>1. The Herschel-Bulkley model will become the Bingham model when the viscosity of a fluid is constant, but for MR fluids, n is typically less than 1, meaning that MR fluids will become thinner as shear rates increase. The constitutive equation of the Casson model is

$$\tau^{\frac{1}{2}} = \tau_0^{\frac{1}{2}} + \eta_\infty^{\frac{1}{2}} \dot{\gamma}^{\frac{1}{2}} \quad (\tau \geq \tau_0) \quad (3)$$

where η_∞ is the Casson viscosity that is usually obtained at high shear rates. The Casson model highlights shear thinning by adding the small behavior index ½. The shear yield stresses in the above three constitutive models are all dynamic yield stress, only related to the magnetic field strength for the MR fluid with a constant mass fraction. As can be seen from these three constitutive equations, the shear stress is related to the shear yield stress, viscosity and shear rate, while the shear yield stress and viscosity are also dependent on magnetic field strength and particle concentration.

Although these three models have been used extensively, there is no research on the application scopes of the models until 2018. Lv *et al.*[20] have a comparative experimental study on the above three models based on a typical commercial MR fluid, and their research well summarizes the application scopes of these models. However, the research is still limited to a typical MR fluid with high particle concentration. With the extensive use of MR fluids, various MR fluids with different particle concentrations have been developed for different working conditions[21-24]. There is also a quest for a better sedimentation rate to prepare MR fluids with lower mass fractions because the optimization process of MR fluids is a game of sedimentation rate and shear stress. Regardless of the variation of MR fluids, the magnetic field strength and mass fraction are always the main determinants of shear stress[25]. Besides, Segovia-Gutierrez *et al*[26] found that the MR effects become completely inconsistent at a specific particle concentration, leading to a fact that some of the above conclusions are no longer applicable. To widely investigate the applicability of the above three constitutive models, this work prepares MR fluids with different particle concentrations. Then, their apparent viscosity and shear stress are measured at different magnetic fields and shear rates. On this basis, the rheological parameters are fitted by the Bingham model, the Herschel-Bulkley model and the Casson model to evaluate their application scopes.

2. Preparation and measurements

2.1 MR fluid preparation

The MR fluid samples tested in the experiments were prepared by mixing the ferromagnetic particles with base carrier fluid. The ferromagnetic particles in MR fluids should have high permeability, magnetization saturation and soft magnetic properties such as quite low hysteresis. Carbonyl iron powder (CIP) produced by BASF was adopted in this work. Table 1 shows its performance parameters.

Table 1 Performance parameters of CIPs by BASF[27]

Fe	C	N	O	Mean particle size D50
97.8%	0.6-0.9%	0.6-0.95	0.3-0.5%	2.0 μm

Both oil-based and water-based MR fluids are reported in previous literature. Compared with the water-based MR fluids, the oil-based MR fluids have a higher viscosity, which effectively prevents MR fluids from sedimentation and the uneven particle distribution caused by centrifugal force in experiments. Besides, the oil will not evaporate under heating, ensuring compositional stability for MR fluids, and it can prevent CIPs from being corroded in water, especially stored for a long time. Silicone oil 47V50 from RHODOSIL with appropriate viscosity (50 mm^2/s at 25 °C) and thermal stability (flashpoint at 280 °C) was adopted in the present work. It should be pointed out that the additives to prevent sedimentation and oxidation are omitted in this work because the MR fluid was tested as soon as it was prepared. Besides, the silicone oil with higher viscosity can help to maintain the stability of the MR fluid without sedimentation. MR fluids with different mass fractions from 10 wt% to 80 wt% were prepared to investigate the influence of particle concentration on shear yield stress. The MR fluid with mass fraction of 90 wt% was no longer flowable and could not be considered as a fluid. Besides, there are no commercially available applications for MR fluids with mass fraction of 90 wt%, so it was not researched in this paper.

2.2 Measurement of MR properties

Anton Paar MCR 301 rotational rheometer was used to measure the properties of the MR fluids. The measurements were carried out in the absence of magnetic field and under an applied magnetic field. In the absence of magnetic field, a concentric cylinder module was applied because this module with a large shear surface shows excellent sensitivity especially when the MR fluids are low viscosity suspensions. Besides, the module can effectively reduce the error caused by the centrifugal force during rotation. The concentric cylinder module is composed of a rotating inner cylinder and a stationary outer cylinder where there is an annular gap of 0.71 mm to hold MR fluids, as shown in Figure 1. The rotating cylinder is made of stainless steel with a rough surface to avoid slip, while the stationary cylinder is made of aluminum. The apparent viscosity and shear stress of MR fluids were measured in the shear range from 0.01 s^{-1} to 1000 s^{-1}.

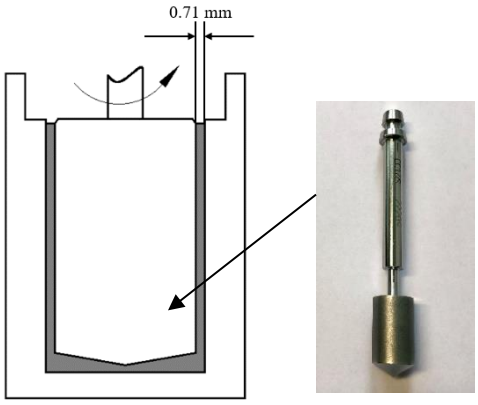

Figure 1. Scheme of concentric cylinder module

The rheometer was equipped with an MRD180/1T MR module to measure the properties of MR fluids under magnetic fields, as illustrated in Figure 2. The MR module is composed of a rotational top plate and a fixed bottom plate where there is a 1 mm gap between the top and bottom plates to hold MR fluids. The MR module also contains an exciting coil that generates a vertical magnetic field through the current control module. The magnetic field passes vertically through the testing gap by upper and lower yokes, as shown by the red arrows in Figure 2. The contact surfaces of both top and bottom plates are made from aluminum with grooves to reduce the errors from wall slip, which is detailed in previous work[28]. The exciting currents were set as 1A, 2A, 3A, 4A and 5A, and the corresponding magnetic field strengths can be obtained from Figure 3. The testing experiments were conducted at 30 ℃ by the circulating water. The apparent viscosity and shear stress of MR fluids were calculated from the flow curve by increasing the shear rate logarithmically from 0.01 to 100 s^{-1} and recording the

resulting shear stress. The MR properties were also measured under shear rates from 0.01 s^{-1} to 3000 s^{-1}, which was used to value the constitutive models under a wider range of shear rates.

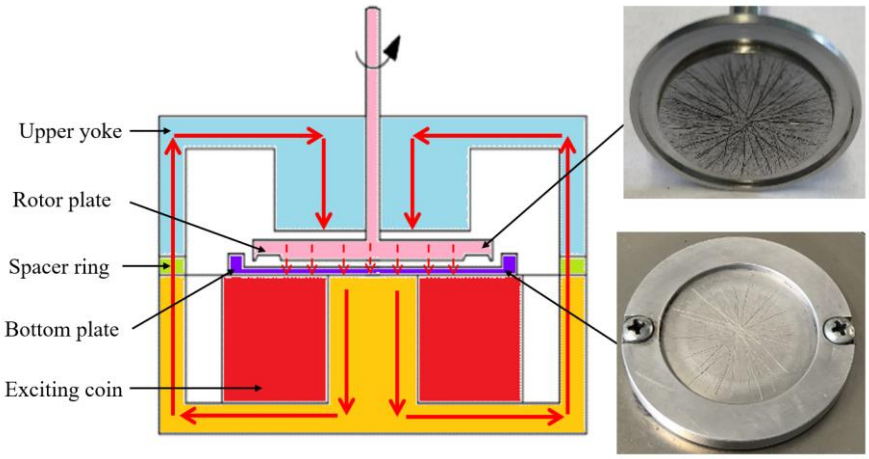

Figure 2. Scheme of MRD180/1T MR module

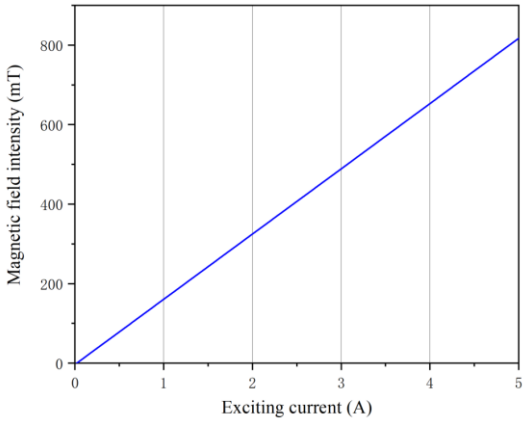

Figure 3. Magnetic field strength curve with exciting current

3. Results and discussion

The three constitutive models are used to fit the experimental data under different magnetic field strengths, mass fractions and shear rate ranges. The coefficient of determination R^2 is applied to indicate the fitting effect, which shows better constitutive model accuracy if R^2 is closer to 1. In this work, four accuracy levels were defined to evaluate the fitting effects: poor level with R^2 more than 0.900 (purple), rough level with R^2 more than 0.900 (red), adequate level with R^2 more than 0.990 (orange), and accurate level with R^2 more than 0.995 (green).

3.1 Different magnetic field strengths

(a) Absence of magnetic field

Figure 4 shows the shear stress of 10 wt% and 80 wt% MR fluids in the absence of magnetic field, as well as the fitting results by Bingham model, Herschel-Bulkley model and Casson model. The 10 wt% MR fluid can be regarded as a Newtonian fluid and its flow curve can be approximated as a straight line passing the origin. At low concentrations, the shear yield stress, no matter which constitutive model is applied, is extremely low (0.003 Pa at 10wt%). The experimental results overlap with the three constitutive models and the coefficient of determination R^2 for all models is 0.999, which is at accurate level. This indicates that the three models describe equally the properties of MR fluids with mass fractions less than 40 wt% where the Bingham model is more practical since it is the simplest model.

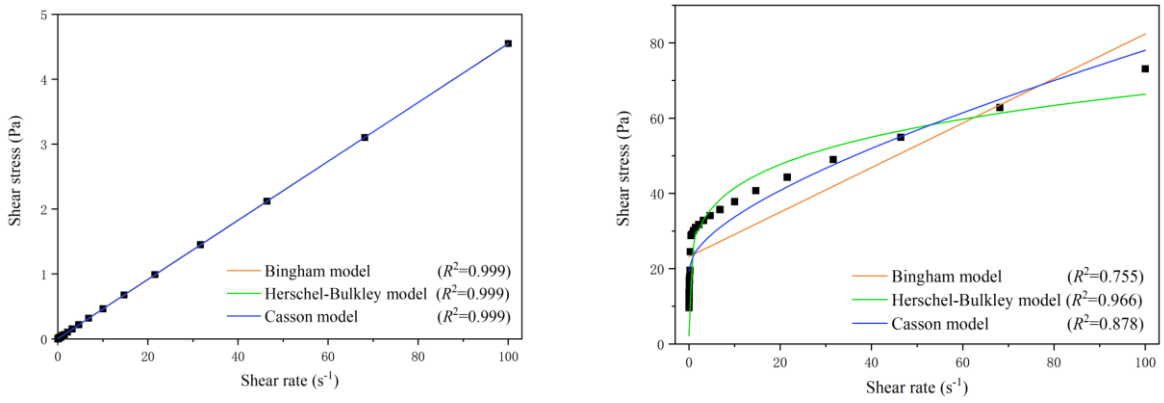

(a) (b)

Figure 4. Constitutive models accuracy of MR fluids with different mass fractions in the absence of magnetic field: (a) 10 wt%, (b) 80 wt%

Table 2 R^2 of three constitutive models in absence of magnetic field

Mass fraction	10 wt%	20 wt%	30 wt%	40 wt%	50 wt%	60 wt%	70 wt%	80 wt%
Bingham model	0.999	0.999	0.999	0.996	0.987	0.947	0.882	0.755
Casson model	0.999	0.999	0.999	0.999	0.999	0.987	0.956	0.878
Herschel-Bulkley model	0.999	0.999	0.999	0.999	0.999	0.988	0.979	0.966

As the mass fraction of MR fluid increases, the correspondence between the models and experimental data weakens. Among the different models, the Bingham model is the worst and it can provide only a rough estimation for the MR fluid properties in the mass fraction range of 40-60 wt%. The coefficient of determination of the Bingham model decreased to 0.882 when the mass fraction was 70 wt% and less than 0.760 with the mass fraction of 80 wt%. The relative error e_r is applied to analyze the Bingham model error:

$$e_r = \frac{\tau_f - \tau_e}{\tau_e} \times 100\% \quad (4)$$

where τ_f is the fitting value of shear stress and τ_e is the experimental value of shear stress. Figure 5 shows the relative error at different shear rates. At extremely low shear rates (black line), the Bingham model is much erroneous and its relative error even exceeds 140%, because the linear Bingham model predicts a higher shear yield stress but the MR fluid at low shear rates is non-Newtonian and the experimental values are much lower. This is the main source of error in the Bingham model. As the shear rate increases, the relative error gradually increases (red line). The MR fluid begins gradually flowing at this point, accompanied by a decrease in viscosity. With the continuous increase in shear rate, the relative error changes within a range (blue line) when the MR fluid has flowed and the viscosity tends to be stable, as shown in Figure 5.

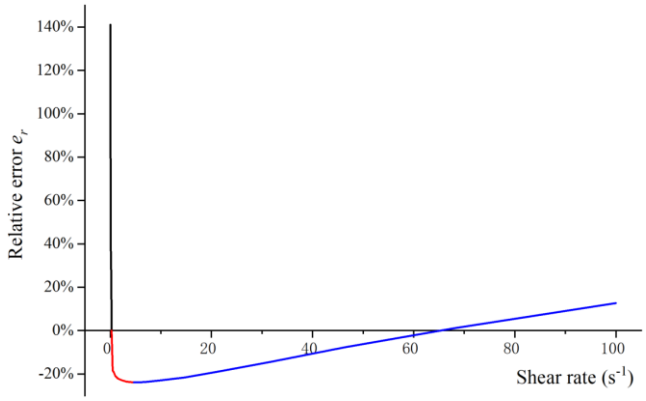

Figure 5 Relative error of 80 wt% MR fluid at different shear rates for the Bingham model

According to the trend in Figure 5, the Bingham model will have an increasing error at higher shear rates, but this assumption is inaccurate. The fitting curve is based on the shear stress corresponding to the shear rate, and there is another Bingham curve in a wider range of shear rates, which will be discussed in section 3.3.

As can be seen from Table 2, the coefficient of determination R^2 of the Casson model and the Herschel-Bulkley model drops from accurate level to rough level, so the Casson model can be applied to describe the properties of MR fluids with the mass fraction of 50-70 wt% because it is also a simpler two-parameter model. As the mass fraction continues to increase, the coefficient of determination R^2 of the Herschel-Bulkley model remains above 0.900, showing an excellent fitting effect, so the Herschel-Bulkley model can be applied to describe the properties of MR fluids with mass fractions above 70 wt%. It should be noted that the MR fluid, even in the absence of magnetic field, is still a non-Newtonian fluid and the non-Newtonian properties are more pronounced with the increase in mass fraction. The shear yield stress of MR fluids with different mass fractions is obtained by the Herschel-Bulkley model that has an excellent fitting effect, as shown in Figure 6.

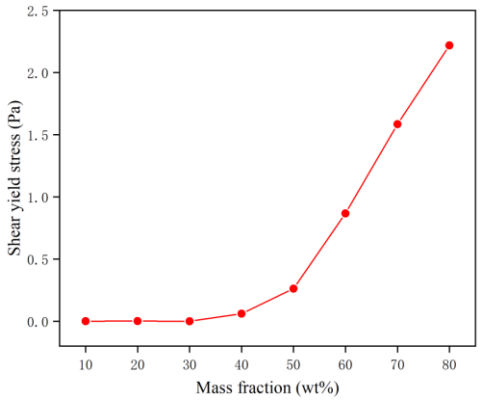

Figure 6 Shear yield stress of MR fluids with different mass fractions at 0 mT

It can be seen from Figure 6 that the MR fluid has shear yield stress even in the absence of magnetic field and the shear yield stress increases gradually with particle concentration so that it cannot be ignored. The shear yield stress, which should appear only when a magnetic field is applied for Newtonian fluids, appears in the absence of magnetic field, indicating that the MR fluids are non-Newtonian fluids even in the absence of magnetic field.

(b) Applied magnetic field

Under the magnetic fields with different strengths, the shear stress of the MR fluid with mass fraction of 60 wt% was fitted to Bingham model, Herschel-Bulkley model and Casson model, as shown in Figure 7.

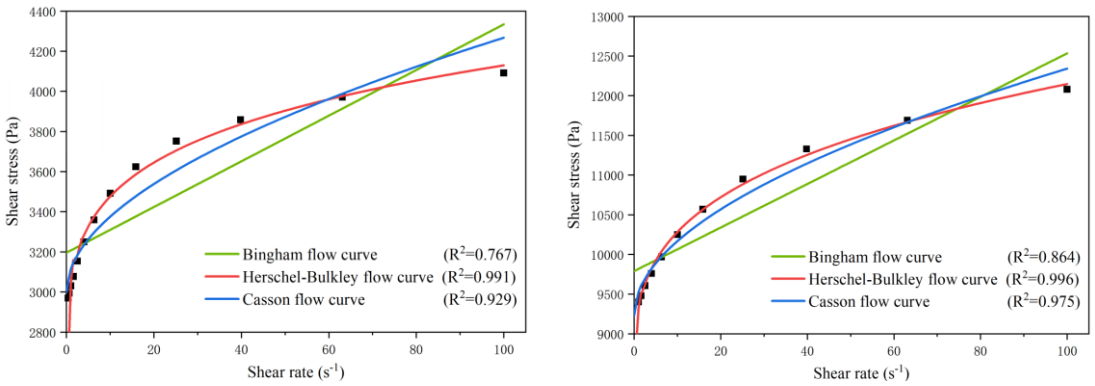

(a) (b)

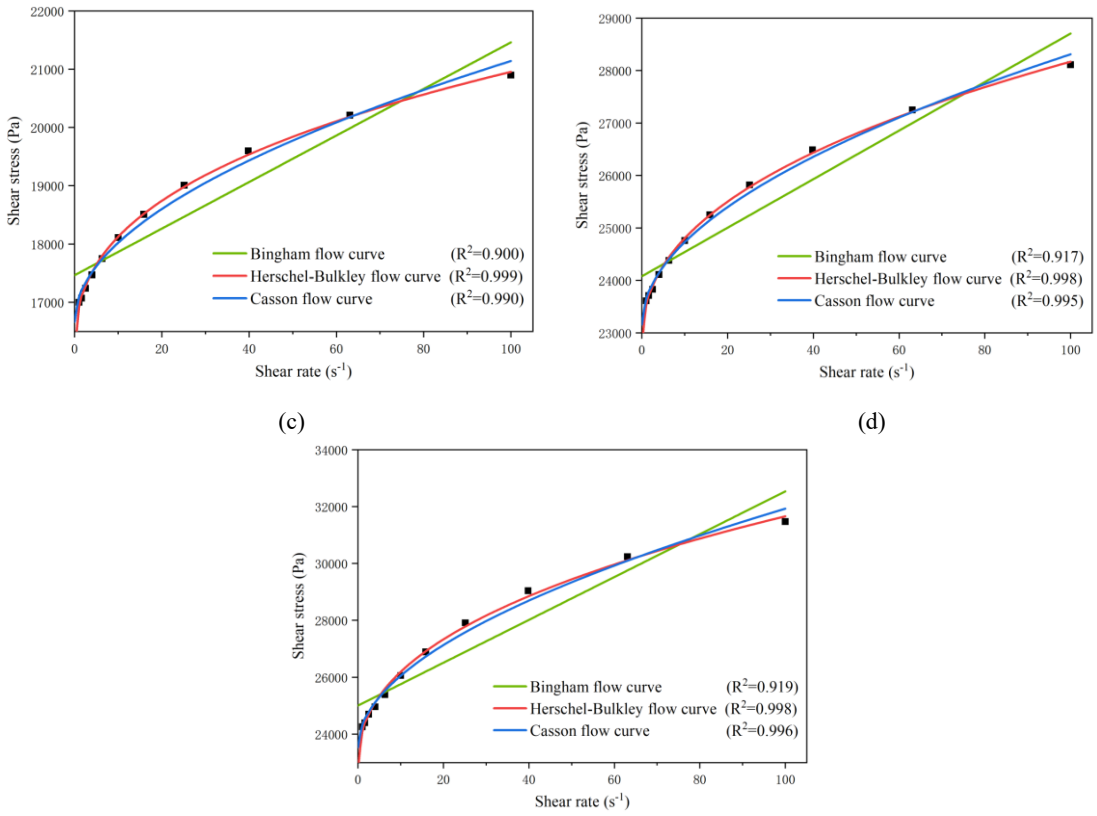

Figure 7 Comparison of the constitutive model accuracy of MR fluids with mass fraction of 60 wt% at different magnetic field strengths: (a) 161 mT, (2) 325 mT, (c) 489 mT, (d) 653 mT, (e) 817 mT

Table 3 R^2 of three constitutive models at different magnetic field strengths

Magnetic field strength	161 mT	325 mT	489 mT	653 mT	817 mT
Bingham model	0.767	0.864	0.900	0.917	0.919
Casson model	0.929	0.975	0.990	0.995	0.996
Herschel-Bulkley model	0.991	0.996	0.999	0.998	0.998

It can be seen from Table 3 that the fitting effects gradually improve as the magnetic field strength increases. As the magnetic field strength increases, the proportion of internal friction is controlled by the magnetic field strengthens as well, which inhibits the non-uniform dispersion of magnetic particles. The shear thinning effect weakens, resulting in less nonlinearity. The Bingham model exhibits poor fitting accuracy under the lower magnetic field strengths because it regards MR fluids after yielding as linear fluids that have constant viscosity. Even though the viscosity of MR fluids changes slowly after yielding, it still decreases at a relatively small rate. The Bingham model ignores the viscosity changes, resulting in a poor fit. The Bingham model can be applied to describe the MR properties under magnetic fields more than 489mT, but it is only at a rough level.

As for the Casson model, it showed better fitting effects under different magnetic field strengths, as shown in Table 3. Compared with the Bingham model, the Casson model describes the shear thinning effects by the rheological index ½, resulting in a better fitting effect. The value of Casson viscosity increases with the magnetic field strength, which is 0.99, 2.25, 2.66, 2.69 and 2.71 at 161mT, 325mT, 489mT, 653mT and 817mT, respectively. It is due to the increase in internal friction controlled by the applied magnetic field, which is similar to the apparent viscosity since the Casson viscosity represents the viscosity of MR fluids at high shear rates. The Casson can be used to describe the properties of MR fluids under the magnetic fields more than 653mT because it is at the same accurate level as the Herschel-Bulkley model and is simpler than the Herschel-Bulkley model. Also,

the Casson model can be used to describe the properties of MR fluids under the magnetic fields of 325-653 mT at an adequate level, as well as less than 325 mT at a rough level.

The Herschel-Bulkley model showed excellent fitting effects under different magnetic field strengths, better than the Bingham model and the Casson model. In the Herschel-Bulkley model, the viscosity coefficient K increases with magnetic field strengths, indicating that the viscosity of MR fluids increases with magnetic field strengths. This is also due to the increase in the internal friction caused by magnetic fields, as stated before. The rheological index n is always less than 1 under different magnetic fields, showing that MR fluids are non-Newtonian fluid with shear thinning. Besides, the rheological index n increases with magnetic field strengths, indicating that the shear thinning weakens with the increase in magnetic field strength. Not surprisingly, as the strength of the magnetic field increases, more particles are arranged in particle chains, which will not distribute unevenly and therefore shear thinning is reduced. The Herschel-Bulkley can be applied to describe the properties of MR fluids under the magnetic fields of 325-653 mT at an accurate level, as well as less than 325 mT at an adequate level.

3.2 Different mass fractions

Figure 8 compares the fit of the Bingham model, the Herschel-Bulkley model and the Casson model for MR fluids with different mass fractions under the magnetic field of 489 mT. All the three constitutive models have good fitting accuracy for MR fluids with lower mass fractions, but it gets worse with the increase in mass fractions.

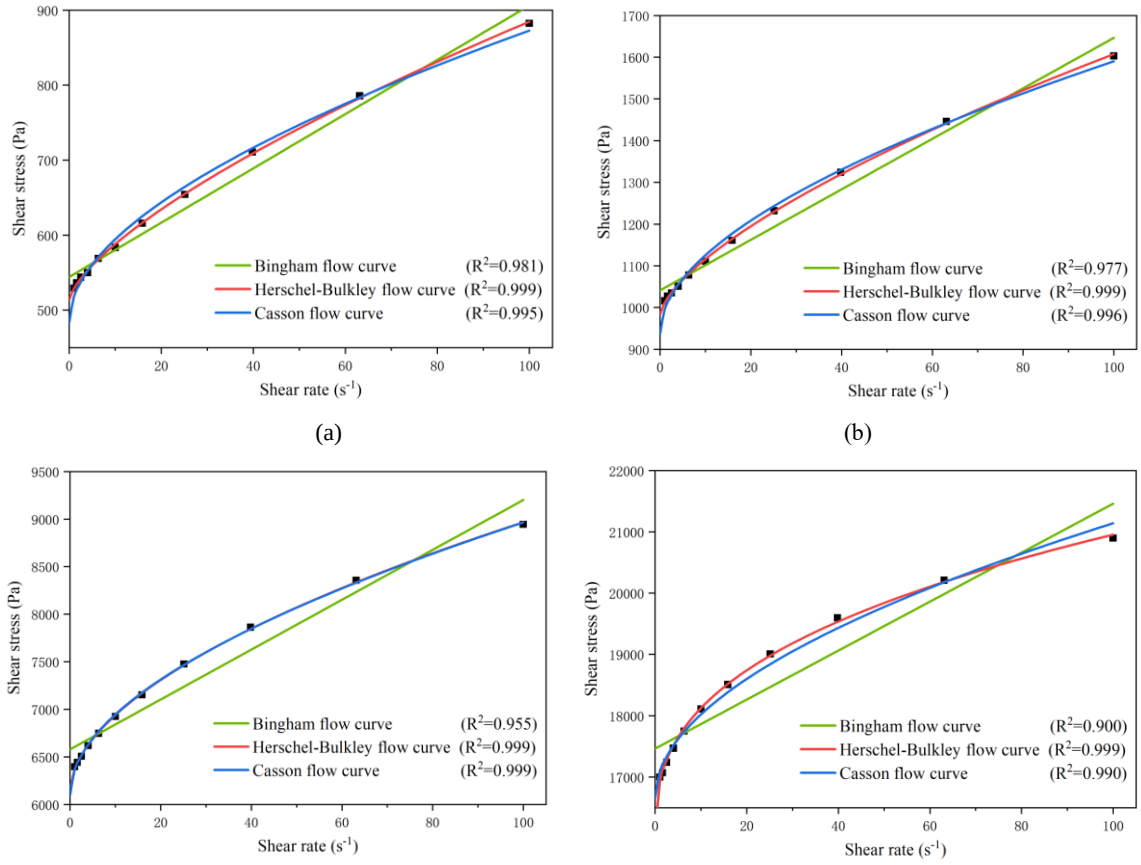

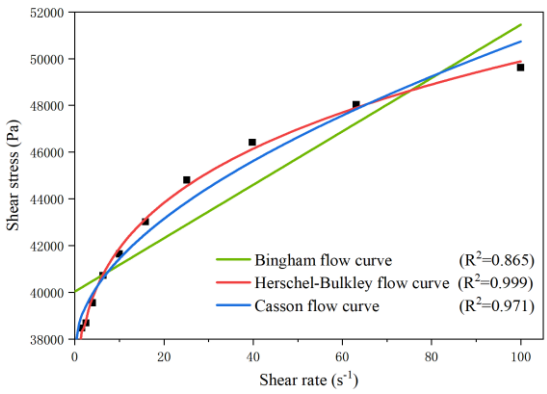

(e)

Figure 8 Comparison of constitutive model accuracy of MR fluids at 489 mT with different mass fractions: (a) 10 wt%, (b) 20 wt%, (c) 40 wt%, (d) 60 wt%, (e) 80 wt%

Table 4 R^2 of three constitutive models for MR fluids with different mass fractions

Mass fraction	10 wt%	20 wt%	30 wt%	40 wt%	50 wt%	60 wt%	70 wt%	80 wt%
Bingham model	0.981	0.977	0.966	0.955	0.925	0.900	0.873	0.865
Casson model	0.995	0.996	0.999	0.999	0.996	0.990	0.975	0.971
Herschel-Bulkley model	0.999	0.999	0.999	0.999	0.999	0.999	0.999	0.999

The Bingham model has good fitting accuracy for MR fluids with lower mass fractions because the shear stress originates from the viscous resistance between carrier fluid molecules while the base carrier fluid is a Newtonian fluid. As a consequence, shear stress increases linearly with shear rate, which is consistent with the Bingham model. For the MR fluid with mass fractions less than 60 wt%, the Bingham model can be used to roughly evaluate its shear stress, as it is the simplest model and all the parameters can be obtained directly through experiments.

Compared to the Bingham model, the Casson model had a better fit with the MR fluids with a medium mass fraction because it takes the shear thinning effect into account. However, it became less accurate with the increase in the mass fractions, as shown in Table 4. As stated above, the Casson model describes the shear thinning effect by the rheological index ½ which, however, can no longer accurately describe the shear thinning of the MR fluids with higher mass fractions. Lv *et al*[20] tried to change the rheological index, finding that the shear stress by the Casson model is not sensitive to the changes in the rheological index. The Casson model is originally applied to describe the properties of the fluids with a lower shear yield stress, such as milk and blood, while the MR fluid has a higher shear yield stress with the increase in mass fraction, which is beyond the scope of the Carson model, leading to a higher error. The Casson viscosity increases nonlinearly with mass fractions and its value is 0.57, 0.86, 1.75, 2.66 and 2.76 for the MR fluids with mass fractions of 20wt%, 40wt%, 60wt% and 80wt%, respectively. The Casson model can be applied to describe the properties of MR fluids with mass fractions less than 50 wt% since it is at the same accurate level as the Herschel-Bulkley model and it is simpler. Also, the Casson can be used to describe the properties of MR fluids with mass fractions of 50-70 wt% at an adequate level, as well as more than 70 wt% at a rough level.

The Herschel-Bulkley model showed excellent accuracy in fitting the flow curve of MR fluids with different mass fractions, better than the Bingham model and the Casson model. No matter what the mass fraction of MR fluid is, the coefficient of determination R^2 of the Herschel-Bulkley model is always at an accurate level, especially at the mass fractions than 60 wt%. As stated in section 3.2.1, the Herschel-Bulkley model can well describe the properties of MR fluids at low shear rates, thus showing better accuracy. The viscosity coefficient K in the Herschel-Bulkley model increases with mass fraction, indicating that the MR fluids become thinker, which

is also due to the increased internal friction from more particle contacts. The rheological index n is always less than 1 for the MR fluids with different mass fractions, which shows that the MR fluids are all shear thinning fluids. Besides, the higher mass fraction will lead to a smaller rheological index n that means a more serious shear thinning effect.

3.3 Different shear rate ranges

Figure 9 compares the fitting accuracy of the Bingham model, the Herschel-Bulkley model and the Casson model in a wider range of shear rates. The MR fluid with mass fraction of 60 wt% was tested under the magnetic field of 489 mT.

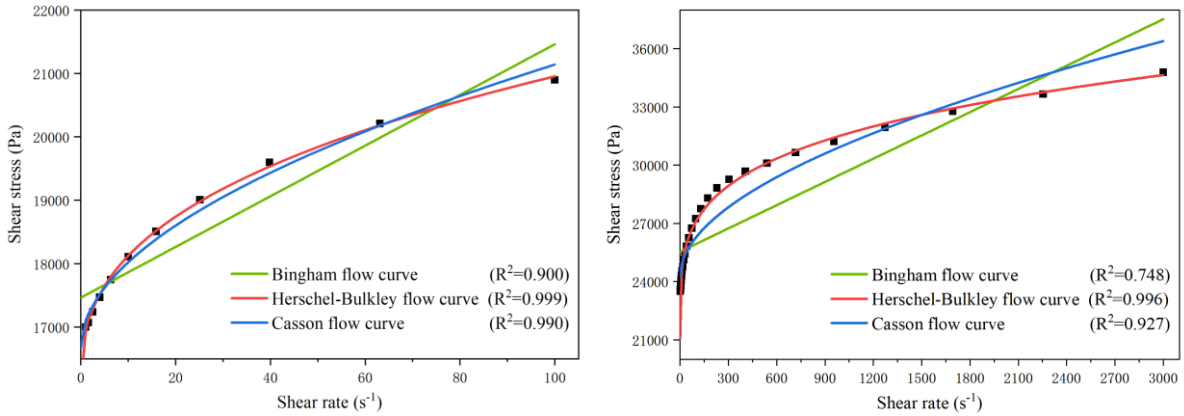

(a) (b)

Figure 9 Comparison of constitutive model accuracy of MR fluids in different shear rate ranges: (a) 100 s^{-1}, (b) 3000 s^{-1}

As the range of shear rate increases, the Bingham model is no longer applicable and its R^2 is only 0.748 in the range from 0 to 3000s^{-1}. It is intuitively clear from Figure 9(b) that the error in the Bingham model is not limited to the low shear rates. At this point, the MR fluid distributes unevenly, resulting in serious shear thinning. The Carson model still performs well and its R^2 is 0.927 in the range from 0 to 3000 s^{-1}. The Casson viscosity η_∞ decreased as the shear rate increased, indicating that the MR fluids become thinner with the increase in shear rate. Also, higher mass fractions lead to an obvious decrease in Casson viscosity η_∞. The fitting effect of the Herschel-Bulkley model stays excellent for wider shear rate range, which is due to the fact that the Herschel-Bulkley curve is more realistic at low shear rates. As stated in section 3.1, increasing magnetic field strength will inhibit the shear thinning effect, but the shear thinning effect from high-rate shearing is even stronger than the inhibition from increasing the magnetic field strength.

3.4 Shear yield stress

In the three constitutive models, whether the two-parameter Bingham model and the Casson model or the three-parameter Herschel-Bulkley model, another important parameter is the shear yield stress that reflects the strength of the MR effect. The shear yield stress is generally considered to be related only to the magnetic field strength. However, the shear yield stress value is not the same when the flow curve is fitted by different constitutive models. Figure 10 compares the shear yield stresses by the three constitutive models under different working conditions.

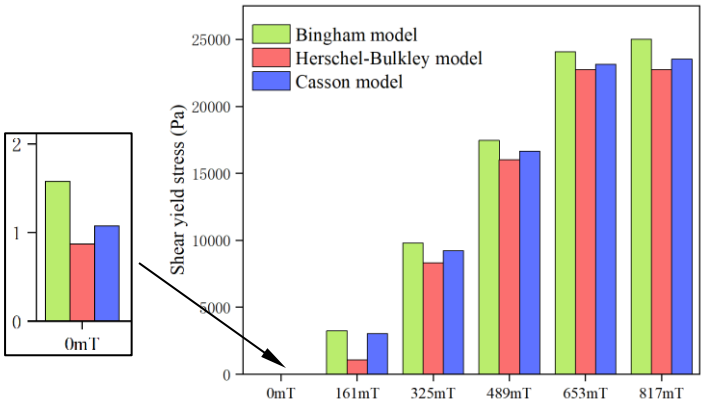

(a)

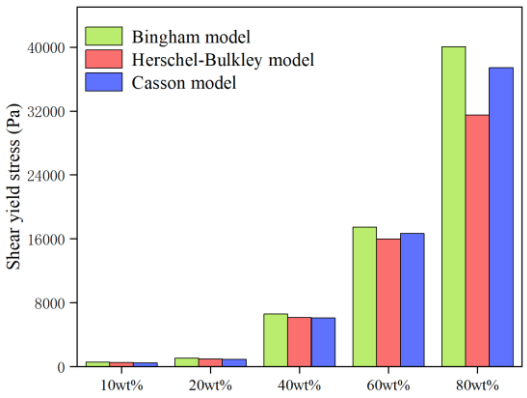

(b)

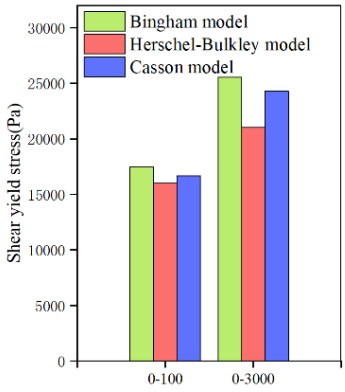

(c)

Figure 10 Shear yield stress by three constitutive models: (a) different magnetic field strengths at 60 wt%, (b) different mass fractions at 489 mT, (c) different shear rate ranges at 60 wt% and 489 mT

The shear yield stress from the Herschel-Bulkley model is usually the smallest, followed by the Casson model and the Bingham model. Further, the difference of shear yield stresses by the three constitutive models is higher at lower magnetic field strengths, higher mass fractions and wider shear rate ranges. The maximum difference of shear yield stress between the Bingham model and the Herschel-Bulkley model is up to 205% at 161 mT, as shown in Figure 10(a). The maximum difference value between the above models is 8500 Pa for 80wt% MR fluid, as shown in Figure 10(b). Even for the same MR fluid and same model, the obtained shear yield stress is different by fitting the flow curve in different shear rate ranges, as shown in Figure 10(c). A higher shear yield stress is obtained in a wider shear rate range.

The order of the estimated valu es from different models can be explained by the characteristics of MR fluids and the three flow curves, as shown in Figures 18, 19 and 20. As stated in Section 3.1, the lower-strength magnetic fields, higher mass fractions and wider shear rate range will lead to a serious shear thinning where the fitting effects differentiate. The linear Bingham flow curve sets a higher shear yield stress to fit the shear stress at higher shear rates, and the rheological index ½ in the Casson model keeps it also higher than the experimental value. However, the flexible rheological index n in the three-parameter Herschel-Bulkley model extends the curve downwards at low shear rates, which is consistent with the properties of real MR fluids. As a consequence, the shear yield stress by the Herschel-Bulkley model is relatively low resulting in a better fit than the other two models.

As the shear yield stress is quite different by different models, it is important to choose an accurate model to calculate the shear yield stress. Although the shear yield stress is different from the three constitutive models, it has the same increasing trend with the increase in magnetic field strength and mass fraction.

4. Conclusions

In the absence of a magnetic field, the MR fluids with mass fractions less than 40 wt% can be regarded as Newtonian fluids, since they reflect mainly the properties of the Newtonian base carrier fluid. Therefore, the Bingham model, the Herschel-Bulkley model and the Casson model can well characterize their properties. With the increase in mass fractions, the MR fluids become more nonlinear turning into non-Newtonian fluids and the constitutive models start to deviate from the real shear stress.

The errors of constitutive models originate from the shear thinning of MR fluids, which is more likely to occur for the MR fluids with higher mass fractions, while a stronger magnetic field will inhibit it. However, the shear thinning effect from high-rate shearing is stronger than the inhibition from increasing the magnetic field strength. The error of the Bingham model appears at extremely low shear rates (below 1 s^{-1}) and the model is suitable only for MR fluids with low mass fractions (less than 40 wt%) under strong magnetic fields (higher than 489 mT) and low shear-rate range. At this time, the coefficient of determination R^2 of the Bingham model is higher than 0.900. The Casson model can be applied to describe the properties of MR fluids with low and moderate mass fractions (less than 60 wt%). It is also applicable under low-strength magnetic fields and in a wider shear rate range. The R^2 value of the Casson model is 0.990 with the accuracy improved by an order of magnitude when compared with the Bingham model. The Herschel-Bulkley model can well describe the properties of MR fluids at extremely low shear rates, resulting in an excellent fitting accuracy with the coefficient of determination R^2 higher than 0.995. Therefore, the Herschel-Bulkley is applicable to MR fluids with different mass fractions at various magnetic field strengths and shear rate ranges. The shear yield stress is maximum when obtained from the Bingham model, followed by the Carson model, while the Herschel-Bulkley model predicts the smallest value. The difference of shear yield stress by the three constitutive models is even higher at lower-strength magnetic fields, higher mass fractions and wider shear rate range.

This paper also provides a guidance for selecting a proper model to predict the properties of MR fluids, especially when the MR fluids with different mass fractions are prepared and the MR devices are controlled in different precisions.

Compliance with ethical standards

Conflicts of interest: The authors declare that there is no conflict of interest regarding the publication of this paper.

Acknowledgements

This research was supported by the National Natural Science Foundation of China (52074272, 51875560 and 52005426), Natural Science Foundation of Jiangsu Province (BK20190155), Postgraduate Research & Innovation Projects of Jiangsu Province (KYCX21_2185), Postgraduate Research & Innovation Projects of CUMT (2021WLKXJ045) and Priority Academic Program Development of Jiangsu Higher Education Institutions.

Data Availability

The main data that support the findings of this study are available within the article. Complementary data that support the findings of this study are available from the corresponding author upon reasonable request.

References

1. Oladapo BI, Muhammad MA, Adebiyi VA, Oluwole B, Usman H. Model hybrid magnetorheological damping prediction in machine tools. Eng Struct 2020, **213**.
2. Wu XF, Huang CH, Tian ZZ, Ji JJ. Development of a novel magnetorheological fluids transmission device for high-power applications. Smart Mater Struct 2019, **28**(5).
3. Kumari C, Chak SK, Vani VV. Experimental investigations and optimization of machining parameters

for Magneto-rheological Abrasive Honing process. Mater Manuf Process 2020.
4. Kubik M, Pavlicek D, Machacek O, Strecker Z, Roupec J. A magnetorheological fluid shaft seal with low friction torque. Smart Mater Struct 2019, **28**(4).
5. Binyet EM, Chang JY. Magnetohydrodynamics modelling of a permanent magnets activated MRF clutch-brake. Microsyst Technol 2020.
6. Park BJ, Fang FF, Choi HJ. Magnetorheology: materials and application. Soft Matter 2010, **6**(21)**:** 5246-5253.
7. Wang KJ, Dong XM, Li JL, Shi KY, Li KJ. Effects of Silicone Oil Viscosity and Carbonyl Iron Particle Weight Fraction and Size on Yield Stress for Magnetorheological Grease Based on a New Preparation Technique. Materials 2019, **12**(11).
8. Rabbani Y, Hajinajaf N, Tavakoli O. An experimental study on stability and rheological properties of magnetorheological fluid using iron nanoparticle core-shell structured by cellulose. J Therm Anal Calorim 2019, **135**(3)**:** 1687-1697.
9. Williams EW, Rigby SG, Sproston JL, Stanway R. Electrorheological Fluids Applied to an Automotive Engine Mount. J Non-Newton Fluid 1993, **47:** 221-238.
10. Choi YT, Bitman L, Wereley NM. Nondimensional analysis of electrorheological dampers using an eyring constitutive relationship. J Intel Mat Syst Str 2005, **16**(5)**:** 383-394.
11. Papanastasiou TC. Flows of materials with yield. J Rheol 1987, **31**(5)**:** 385-404.
12. Rao MA, Bourne MC, Cooley HJ. Flow Properties of Tomato Concentrates. J Texture Stud 1981, **12**(4)**:** 521-538.
13. Pelegrine DH, Silva FC, Gasparetto CA. Rheological behavior of pineapple and mango pulps. Lebensm-Wiss Technol 2002, **35**(8)**:** 645-648.
14. Cvek M, Mrlik M, Pavlinek V. A rheological evaluation of steady shear magnetorheological flow behavior using three-parameter viscoplastic models. J Rheol 2016, **60**(4)**:** 687-694.
15. Rosensweig RE. On Magnetorheology and Electrorheology as States of Unsymmetric Stress. J Rheol 1995, **39**(1)**:** 179-192.
16. Saha P, Mukherjee S, Mandal K. Rheological response of magnetic fluid containing Fe3O4 nano structures. J Magn Magn Mater 2019, **484:** 324-328.
17. Desai RM, Acharya S, Jamadar MEH, Kumar H, Joladarashi S, Sekaran SCR. Synthesis of magnetorheological fluid and its application in a twin-tube valve mode automotive damper. P I Mech Eng L-J Mat 2020, **234**(7)**:** 1001-1016.
18. Malik MY, Khan M, Salahuddin T, Khan I. Variable viscosity and MHD flow in Casson fluid with Cattaneo-Christov heat flux model: Using Keller box method. Eng Sci Technol 2016, **19**(4)**:** 1985-1992.
19. Blair GS, Hening J, Wagstaff A. The Flow of Cream through Narrow Glass Tubes. Journal of physical chemistry 1939, **43**(7)**:** 853-864.
20. Lv HZ, Chen R, Zhang SS. Comparative experimental study on constitutive mechanical models of magnetorheological fluids. Smart Mater Struct 2018, **27**(11).
21. Chen F, Li HP, Han MM, Tian ZZ, Li AM. Preparation of magnetorheological fluid with excellent sedimentation stability. Mater Manuf Process 2020, **35**(10)**:** 1077-1083.
22. Tian ZZ, Wu XF, Xiaoxingming, Chen F. A Novel Preparation Process for Magnetorheological Fluid with High Working Temperature. J Magn 2019, **24**(4)**:** 634-640.
23. Dorosti AH, Ghatee M, Norouzi M. Preparation and characterization of water-based magnetorheological fluid using wormlike surfactant micelles. J Magn Magn Mater 2020, **498**.
24. Kumar V, Kumar R, Kumar H. Rheological Characterization of Vegetable-Oil-based Magnetorheological Finishing Fluid. Mater Today-Proc 2019, **18:** 3526-3531.

25. Sidpara A, Das M, Jain VK. Rheological Characterization of Magnetorheological Finishing Fluid. Mater Manuf Process 2009, **24**(12)**:** 1467-1478.
26. Segovia-Gutierrez JP, Berli CLA, de Vicente J. Nonlinear viscoelasticity and two-step yielding in magnetorheology: A colloidal gel approach to understand the effect of particle concentration. J Rheol 2012, **56**(6)**:** 1429-1448.
27. www.carbonylironpowder.com
28. Jonkkari I, Kostamo E, Kostamo J, Syrjala S, Pietola M. Effect of the plate surface characteristics and gap height on yield stresses of a magnetorheological fluid. Smart Mater Struct 2012, **21**(7).